Archives of Biochemistry and Biophysics 583 (2015) 36–46

Contents lists available at ScienceDirect

Archives of Biochemistry and Biophysics

journal homepage: www.elsevier.com/ locate/yabbi

Identification of rice Os4BGlu13 as a β-glucosidase which hydrolyzes gibberellin A4 1-O-β-D-glucosyl ester, in addition to tuberonic acid glucoside and salicylic acid derivative glucosides

Yanling Hua [a, b], Watsamon Ekkhara [b, c], Sompong Sansenya [d], Chantragan Srisomsap [e], Sittiruk Roytrakul [f], Wataru Saburi [g], Ryosuke Takeda [g], Hideyuki Matsuura [g], Haruhide Mori [g], James R. Ketudat Cairns [b, c, e, *]

[a] The Center for Scientific and Technological Equipment, Suranaree University of Technology, Nakhon Ratchasima 30000, Thailand
[b] Center for Biomolecular Structure, Function and Application, Suranaree University of Technology, Nakhon Ratchasima 30000, Thailand
[c] School of Biochemistry, Institute of Science, Suranaree University of Technology, Nakhon Ratchasima 30000, Thailand
[d] Department of Chemistry, Faculty of Science, Rajamangala University of Technology, Thanyaburi, Pathun Thani 12110, Thailand
[e] Chulabhorn Research Institute, Bangkok 10210, Thailand
[f] National Center for Genetic Engineering and Biotechnology, Pathum Thani 12120, Thailand
[g] Research Faculty of Agriculture, Hokkaido University, Kita-9, Nishi-9, Kita-ku, Sapporo 060-8589, Japan

ARTICLE INFO

Article history:
Received 11 June 2015
Received in revised form
29 July 2015
Accepted 30 July 2015
Available online 1 August 2015

Keywords:
β-glucosidase
Rice
Gibberellin glucosyl ester
Recombinant expression
Phytohormone conjugates

ABSTRACT

Gibberellin 1-O-β-D-glucose ester hydrolysis activity has been detected in rice seedling extracts, but no enzyme responsible for this activity has ever been purified and identified. Therefore, gibberellin A4 glucosyl ester (GA_4-GE) β-D-glucosidase activity was purified from ten-day rice seedling stems and leaves. The family 1 glycoside hydrolase Os4BGlu13 was identified in the final purification fraction. The Os4BGlu13 cDNA was amplified from rice seedlings and expressed as an N-terminal thioredoxin-tagged fusion protein in *Escherichia coli*. The purified recombinant Os4BGlu13 protein (rOs4BGlu13) had an optimum pH of 4.5, for hydrolysis of *p*-nitrophenyl β-D-glucopyranoside (*p*NPGlc), which was the best substrate identified, with a k_{cat}/K_m of 637 mM^{-1} s^{-1}. rOs4BGlu13 hydrolyzed helicin best among natural glycosides tested (k_{cat}/K_m of 74.4 mM^{-1} s^{-1}). Os4BGlu13 was previously designated tuberonic acid glucoside (TAG) β-glucosidase (TAGG), and here the k_{cat}/K_m of rOsBGlu13 for TAG was 6.68 mM^{-1} s^{-1}, while that for GA_4-GE was 3.63 mM^{-1} s^{-1} and for salicylic acid glucoside (SAG) is 0.88 mM^{-1} s^{-1}. rOs4BGlu13 also hydrolyzed oligosaccharides, with preference for short β-(1 → 3)-linked over β-(1 → 4)-linked glucooligosaccharides. The enzymatic data suggests that Os4BGlu13 may contribute to TAG, SAG, oligosaccharide and GA_4-GE hydrolysis in the rice plant, although helicin or a similar compound may be its primary target.

1. Introduction

Phytohormones serve as chemical messengers to regulate cellular activities, vegetative and reproductive development, and stress responses. These plant hormones include auxins, cytokinins, gibberellins, ethylene and abscisic acid (ABA), brassinosteroids, strigolactones, jasmonates and salicylates. Many of these phytohormones can be conjugated to glucose. Phytohormone glucosyl conjugates are inactive reserve forms of active phytohormones in plants, which can be hydrolyzed to release active phytohormones by β-glucosidases. The β-glucosidases that hydrolyze these conjugates have been found in several plants [1–4].

The gibberellins (GAs) are a class of plant hormones that play important roles in various plant growth phenomena, including seed germination, stem elongation, and flower development. They are highly functionalized diterpenoids and are distributed widely in plants, fungi and bacteria [5–8]. Among the 136 known GAs, only a few of them are biologically active in plants. These include GA_1, GA_3, GA_4, GA_5, GA_6 and GA_7. Gibberellic acid (GA_3), which was the first gibberellin to be structurally characterized, has been widely used to regulate plant growth and development.

* Corresponding author. School of Biochemistry, Institute of Science, Suranaree University of Technology, Nakhon Ratchasima 30000, Thailand.
E-mail address: cairns@sut.ac.th (J.R. Ketudat Cairns).

http://dx.doi.org/10.1016/j.abb.2015.07.021
0003-9861/

The bioactive GAs exist in the plants together with many inactive GAs and their glucosyl conjugates, which may be inactive precursors or inactivation products of the active forms, and are closely regulated by the GA biosynthetic and catabolic pathways [9]. Both 1-*O*-acyl glucosyl esters and glucosides of GAs are found in plants. It has been suggested that GA glucosyl esters are deactivated GAs that can be enzymatically reconverted to active GAs, thus serving as a reserve form of biologically active GAs [10]. The metabolites, [^{13}C]GA_{20}, [^{13}C]GA_{29}, [^{13}C]GA_{20}-13-*O*-glucoside, [^{13}C]GA_{29}-2-*O*-glucoside, [^{13}C]GA_8 and [^{13}C]GA_8-2-*O*-glucoside were identified in the extracts of the seedlings made 24 h after the injection of [^{13}C]GA_{20}-β-D-glucosyl ester into light-grown maize seedlings [11]. This showed that the endogenous hydrolysis of the introduced conjugate and its reconjugation led to the three new glucosides. In rice (*Oryza sativa*), [^{3}H]GA_1, [^{3}H]GA_2, [^{3}H]GA_{34}, the glucosides of [^{3}H]GA_2, [^{3}H]GA_4, [^{3}H]GA_8 and [^{3}H]GA_{34}, and the glucosyl ester of [^{3}H]GA_4 (GA_4-GE) have been found after application of [^{3}H]GA_4 to cell suspension cultures of cv. nipponbare [12].

Beta-glucosidases (β-D-glucopyranoside glucohydrolases, E.C. 3.2.1.21) are essential enzymes in all living organisms and playing important roles in biomass conversion in microorganisms [13], glycolipid metabolism in animals [14], and activation of defense compounds [15,16], phytohormones [17,18], lignin precursors [19], aromatic volatiles [20], and metabolic intermediates [21] in plants. Beta-glucosidases hydrolyze the β-O-glycosidic bond at a non-reducing terminal D-glucosyl moiety through a double-displacement mechanism to release β-D-glucose from glycosides and oligosaccharides. In doing so, they can release glucose blocking groups from their inactive glucosides in plants. To achieve specificity for these various functions, different β-glucosidases must bind to distinct aglycones with a wide variety of structures, in addition to the glucosyl moiety of the substrate. These substrates may include phytohormone glycoconjugates, such as cytokinin glucoside and abscissic acid 1-*O*-glucose ester [3,17]. Recently, two closely related rice glycoside hydrolase family 1 β-glucosidase isoenzymes, Os4BGlu12 and Os4BGlu13, were found to hydrolyze tuberonic acid beta-glucoside (TAG, Fig. 1a), and were designated TAG β-glucosidase 1 (TAGG1) and TAGG2 [4,22].

Although β-glucosidases have been proposed to hydrolyze the GA conjugates to active GAs, the molecular identification of the responsible enzymes and investigation of their modes of action have yet to be reported. Schliemann [1] reported that β-glucosidases extracted from mature rice seeds and seedlings have different hydrolytic activities toward GA_8-2-*O*-glucoside, GA_3-3-*O*-glucoside and 1-*O*-GA_3-glucosyl ester, but purification and characterization of the β-glucosidase activities was not performed. In this study, we extracted a family 1 glycoside hydrolase, Os4BGlu13, which has relatively high activity to hydrolyze GA_4-GE (Fig. 1b). We also expressed Os4BGlu13 in *Escherichia coli*, purified the expressed rOs4BGlu13 and characterized its hydrolytic activities to natural and synthetic glycosides.

2. Materials and methods

2.1. Materials

Rice (*O. sativa* cv. Suphan buri 1) was grown in a field in Sikiu district, Nakhon Ratchasima province, Thailand, during December, 2011. After 10 days, seedling stems and leaves were collected and used for protein purification.

GA_4-GE was synthesized from GA_4 (Jiangsu Fengyuan Bioengineering Co.Ltd, P. R. China) following the previously described methods [23,24]. The acetylated and deacetylated GA_4-GE were confirmed by NMR spectra on a 300 MHz NMR spectrometer with a Varian 300 ID/PFG probe at a frequency of 299.986 MHz (Unity INOVA, Varian, USA). Tuberonic acid β-D-glucopyranoside (TAG) and salicylic acid β-D-glucoside (SAG) were synthesized as

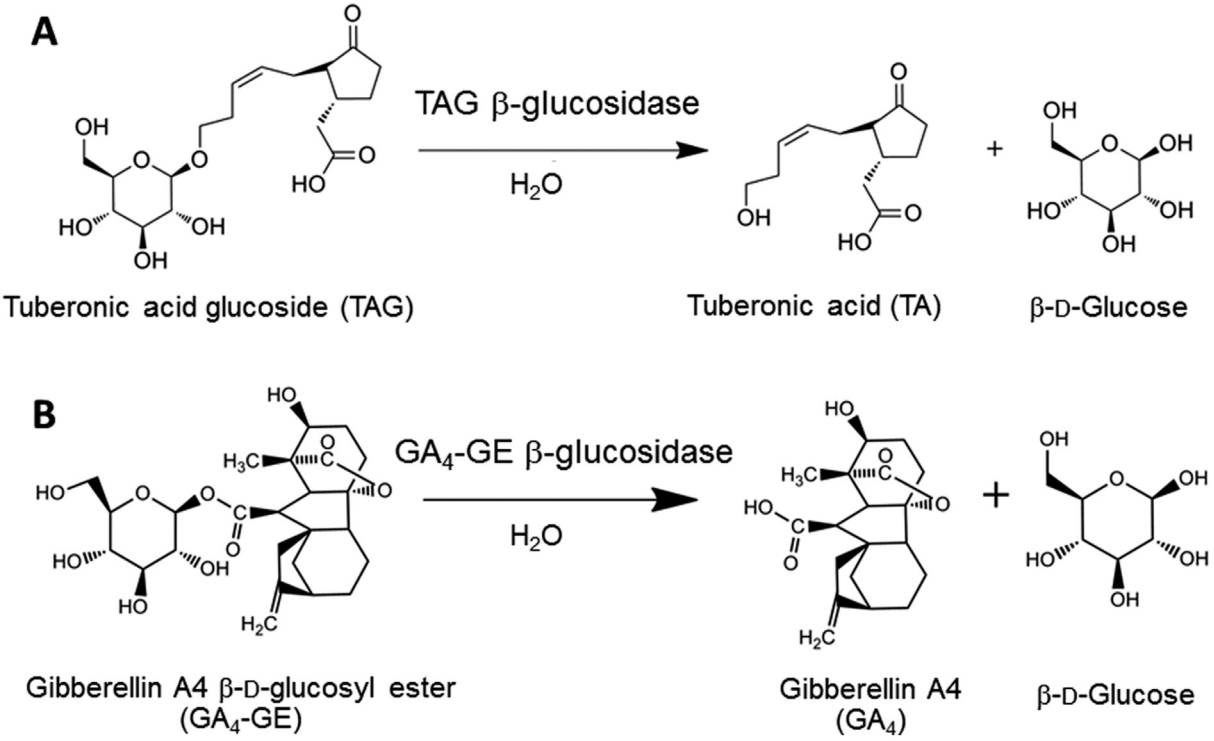

Fig. 1. Reactions of phytohormone β-glucosidases of interest. A) Tuberonic acid β-glucoside is hydrolyzed by TAG β-glucosidase 1 (TAGG1) to release tuberonic acid and glucose. B) GA_4-GE is hydrolyzed by gibberellin glucose ester β-glucosidase to release GA_4 and glucose.

previously described [25,26]. Other glycoside substrates were purchased from Sigma–Aldrich (St. Louis, MO, USA).

2.2. Extraction and purification of β-glucosidase from 10-day-old rice seedlings

Ten kilograms of 10-day-old rice seedling stems and leaves were cut to small pieces with a blender, and the protein was extracted with McIlvaine buffer (0.1 M citric acid–0.2 M disodium hydrogen phosphate (Na_2HPO_4), pH 5.0) supplemented with 1 mM phenylmethylsulfonyl fluoride (PMSF) at 4 °C overnight. The ratio of seedlings and buffer was 100 g per 600 ml. A crude extract was obtained by filtering and centrifugation at 12,000 × g for 20 min at 4 °C. The protein was precipitated with 80% saturated ammonium sulfate $(NH_4)_2SO_4$ and the pellet was collected by centrifugation.

The protein pellet was redissolved in 4-fold diluted McIlvaine buffer, pH 5, (buffer A) and dialyzed overnight against buffer A twice, then centrifuged to remove precipitate. The supernatant was tested for hydrolysis activities toward *p*-nitrophenyl–β-D-glucopyranoside (*p*NPGlc) and GA_4-GE. The dialyzed protein was loaded onto a CM-Sepharose fast flow column (HiPrep CM FF 16/10, 20 ml, GE Healthcare, Little Chalfont, UK) equilibrated with buffer A. The unbound proteins were washed out with buffer A and the bound proteins were eluted with a linear gradient of 0–1.0 M sodium chloride (NaCl) in buffer A at a flow rate of 2.0 ml/min (200 ml total). The fractions were collected and tested for hydrolysis activities toward *p*NPGlc and GA_4-GE. The fractions with activities to GA_4-GE were pooled and precipitated with $(NH_4)_2SO_4$ (80% saturation), followed by centrifugation at 16,000 × g for 20 min at 4 °C, then dialyzed against 20 mM Tris(hydroxymethyl) aminomethane hydrochloride (Tris–HCl), pH 7, containing 0.5 M NaCl (buffer B).

The dialyzed protein was loaded onto a packed Con A-Sepharose 4B column (C10/20, 10 ml, GE Healthcare) equilibrated with buffer B. The column was washed with 4 column volumes (CV) of buffer B, and then eluted with 4 CV of 0.5 M D-mannose in buffer B. The collected fractions were tested for hydrolysis of *p*NPGlc and the active fractions were combined and concentrated with centrifugal filters (Amicon Ultra, regenerated cellulose, 30,000 MWCO) at 700 × g, 4 °C. The buffer of the concentrate was exchanged twice with 4-fold diluted McIlvaine buffer, pH 7, containing 0.2 M NaCl (buffer C), before testing activity with GA_4-GE and further purification by gel-filtration chromatography.

The concentrated protein obtained by the Con A-Sepharose column chromatography was loaded to a Superdex-75 gel-filtration column (XK 26/40, 150 ml, GE Healthcare) equilibrated with buffer C on an ÄKTA Protein Purifier system (GE Healthcare), and eluted at a flow rate of 1.0 ml/min. The fractions were tested for *p*NPGlc and GA_4-GE hydrolysis activities and their purities checked with sodium dodecyl sulfate polyacrylamide gel electrophoresis (SDS-PAGE). The active fractions were pooled and concentrated, and then the buffer was exchanged with buffer A.

The concentrated protein from the Superdex-75 gel-filtration column was loaded onto a 1 ml HiTrap SP Sepharose XL column (GE Healthcare) equilibrated with buffer A on an ÄKTA Protein Purifier system. The column was eluted with a linear gradient of 0–1.0 M NaCl in buffer A at a flow rate of 1.0 ml/min. The fractions with hydrolysis activities were concentrated and the buffer exchanged with 50 mM sodium phosphate buffer, pH 7, containing 1.7 M $(NH_4)_2SO_4$ (buffer D), by centrifugal filtration as described above.

The protein from SP chromatography was loaded onto a 1 ml HiTrap octyl FF column (Sepharose 4, GE Healthcare), which was pre-equilibrated with buffer D. The protein was eluted with a linear gradient of 1.7–0 M $(NH_4)_2SO_4$ in 50 mM sodium phosphate buffer, pH 7.0. The buffer of the collected fractions was exchanged twice with buffer A by centrifugal filtration, as described above, before they were tested for *p*NPGlc and GA_4-GE hydrolysis.

Finally, the active fractions were pooled and loaded to a Superdex-200 gel-filtration column (10/300, 24 ml, GE Healthcare) which was equilibrated with buffer C, and eluted with the same buffer. The protein concentrations and GA_4-GE hydrolysis activities of the fractions were measured, and their purity checked with SDS-PAGE.

2.3. Identification of β-glucosidases with LC-MS

The protein from the Superdex-200 column chromatography was separated by 8% SDS-PAGE, and the gel stained with Coomassie brilliant blue R-250. The two main Coomassie-brilliant-blue-stained bands were excised separately and destained with 25 mM ammonium bicarbonate (NH_4HCO_3)/50% methanol (v/v) and washed with water followed by 100% acetonitrile (ACN). Then the gel plugs were dried at room temperature and disulfide bonds were reduced by reaction with 10 mM dithiothreitol in 10 mM NH_4HCO_3. After removal of the dithiothreitol solution, 20 μl of 100 mM iodoacetamide in 10 mM NH_4HCO_3 was added to the gels, which were then kept in the dark at room temperature for 1 h, and washed twice with 200 μl of 100% ACN.

The gels were infiltrated with twenty microliters of 10 ng/μl trypsin (Promega, sequencing grade) and incubated at room temperature for 20 min, then at 37 °C for 3 h. Thirty microliters of 50% ACN/0.1% formic acid (v/v) was added to the sample, and the resulting peptides were extracted by shaking at room temperature for 10 min. The extracted solution was dried at 40 °C overnight. The samples were kept at −80 °C until analysis.

The separation of tryptic peptides was performed with a NanoAcquity system (Waters Corp., Milford, MA, USA) equipped with a Symmetry C_{18} 5 μm, 180 μm × 20 mm trap column and a BEH130C_{18} 1.7 μm, 100 μm × 100 mm analytical reverse phase column (Waters Corp., Milford, MA, USA). Analysis of tryptic peptides was performed on a SYNAPT™ HDMS mass spectrometer (Waters Corp., Manchester, UK). All analyses were performed in positive ion nanoelectrospray mode. The peptides were separated with a gradient of 15–50% acetonitrile in 0.1% formic acid over 15 min at a flow rate of 600 nl/min, then the column was washed 3-min with 80% acetonitrile, 0.1% formic acid. The column temperature was maintained at 35 °C. The time-of-flight analyzer of the mass spectrometer was externally calibrated with [Glu^1]fibrinopeptide B from *m*/*z* 50 to 1600 with acquisition lock mass corrected using the monoisotopic mass of the doubly charged precursor of [Glu^1]fibrinopeptide B. The MS/MS survey was over the range of 50–1990 Da and the scan time was 0.5 s. The peptide mass results were used in a MASCOT search of the Genbank *non-redundant* (nr) protein database.

2.4. Determination of β-glucosidase activity from protein fractions

The activities of protein fractions to hydrolyze *p*NPGlc were tested in a manner similar to previously published methods [27–30]. Aliquots of enzyme solutions were incubated with 4 mM *p*NPGlc in 50 mM sodium acetate (NaOAc) buffer, pH 5.0, (total reaction volume 50 μl) at 30 °C for 20 min. The reactions were stopped by adding 150 μl of 2 M sodium carbonate (Na_2CO_3). The released *p*-nitrophenol (*p*NP) was quantified by measuring the absorbance at 405 nm (A_{405}) with a microplate reader (Thermo Labsystems, Helsinki, Finland), and comparing it to that of a *p*NP standard curve. The hydrolysis of GA_4-GE was determined by a similar reaction in 50 mM NaOAc, followed with a peroxidase/glucose oxidase-based glucose assay (PGO assay, Sigma–Aldrich), as previously described [24]. In all cases, control reactions

incubated without β-glucosidase enzyme served as blanks. Protein concentrations were determined with a Bio-Rad Bradford assay with bovine serum albumin (BSA) as a standard.

2.5. Cloning of Os4BGlu13

Total mRNA was extracted from 7 week old rice cv. KDML105 seedlings with a Spectrum Plant RNA extraction kit (Sigma–Aldrich). The mRNA was reverse transcribed from a poly dT18 primer with Superscript III reverse transcriptase (Invitrogen, Carlsbad, CA, USA) and the derived cDNA used as a template for PCR. The Os4BGlu13 cDNA was amplified by nested PCR with the Os4BGlu13StartF (5′-ATCCTTGCACAGCCATATGTC-3′) and Os4BGlu13_3pR (5′-AGCCGTGCTCAA GGAGAATCG-3′) primers in the first round and Os4BGlu13MatStNcoI (5′-CACCATG-GAGCCGCCGCCGATCAG-3′) and Os4BGlu13StopR (CCAAGCTT-CATTTCTGGAGGAACTCCTTG) primers in the second round. The final product was gel-purified, digested with *Nco*I and *Hin*dIII, cloned into the corresponding sites in the pET32a(+) expression vector (Novagen, Merck-Millipore, Darmstadt, Germany), and sequenced thoroughly in both directions by automated DNA sequencing (Macrogen, Seoul, Korea).

2.6. Recombinant expression and purification of Os4BGlu13

The recombinant pET32a/Os4BGlu13 plasmids were introduced into *E. coli* strain Rosetta-gami(DE3). The transformants were selected on an LB plate containing 12.5 μg/ml chloramphenicol and 50 μg/ml ampicillin at 37 °C overnight. For expression, these cells were grown continuously at 37 °C with shaking at 220 rpm until the OD_{600} reached 0.4–0.6. Protein expression was induced with 0.2 mM IPTG (final concentration) at 20 °C for 18 h. Cells were collected by centrifugation at 2240 × g for 30 min at 4 °C and the pellet was stored at −80 °C until protein extraction. The pellets were thawed at room temperature. Cells were resuspended with extraction buffer (20 mM Tris–HCl, pH 8.0, 600 μg/ml lysozyme, 1% Triton-X100, 0.1 mM PMSF, 5 μg/ml DNase I and 0.1 mg/ml soybean trypsin inhibitor) and incubated at room temperature for 30 min. Soluble proteins were separated from cell debris by centrifugation at 12,000 × g for 10 min at 4 °C.

Recombinantly expressed Os4BGlu13 (rOs4BGlu13) was purified with 2 steps of immobilized metal affinity chromatography (IMAC) on GE IMAC resin (GE Healthcare) bound with cobalt. The crude protein was mixed with IMAC resin pre-equilibrated with equilibration buffer (20 mM Tris–HCl, pH 8.0, and 150 mM NaCl) at 4 °C for 30 min. The resin with crude protein was loaded into a column and loosely bound proteins were washed out with 5 CV of equilibration buffer, 5 CV of 5 mM imidazole in equilibration buffer and 5 CV of 10 mM imidazole in equilibration buffer. The bound proteins were eluted with 5 CV of 250 mM imidazole in equilibration buffer and 5 CV of 500 mM imidazole in equilibration buffer. The fractions with activity were combined, concentrated and imidazole removed by centrifugal ultrafiltration (Amico Ultra, 30k MWCO) at 700 × g, 4 °C; and the buffer exchanged with 50 mM Tris–HCl, pH 8.0, at 4 °C. The concentrated proteins from the 1st IMAC step were incubated with enterokinase (New England Biolabs), with a ratio of 0.01 μg enterokinase per 10 mg of protein at 20 °C for 20 h to cut off the N-terminal thioredoxin, His_6 and S tags.

The N-terminal thioredoxin, His_6 and S tags were removed with a second IMAC purification, in which the unbound proteins were washed out with 10 CV of equilibration buffer, 10 CV of 5 mM imidazole in equilibration buffer, and 10 CV of 10 mM imidazole in equilibration buffer, respectively. The flow-through and wash fractions containing β-glucosidase activity were combined, concentrated and depleted of imidazole by centrifugal ultrafiltration (Amico Ultra, 30k MWCO) at 700 × g, 4 °C.

2.7. Determination of pH optimum for Os4BGlu13

The optimum pH of rOs4BGlu13 hydrolysis of *p*NPGlc was determined by incubating 0.4 μg of enzyme with 1 mM *p*NPGlc in 80 μl of 100 mM McIlvaine buffers [31], pH 2.5 to 8.0 in 0.5-pH-unit increments (total reaction volume 100 μl), at 30 °C for 10 min. The reactions were stopped by adding 100 μl of 2 M sodium carbonate. The released *p*NP was quantified as described for activity determination.

2.8. Measurement of hydrolysis activities of Os4BGlu13 toward natural and synthetic glycosides

The kinetic parameters of rOs4BGlu13 with natural and synthetic glycosides were determined by the method for determination of β-glucosidase activity for extracted protein fractions, but variable reaction times, enzyme amounts and substrate concentrations were tested to obtain the initial velocities.

For *p*NP glycosides substrates *p*NPGlc, *p*NP-β-D-galactoside, *p*NP-β-D-fucoside, *p*NP-β-D-mannoside and *o*NP-β-D-glucoside, 0.005–1.0 μg of rOs4BGlu13 were incubated with concentrations of substrates that bracketed the apparent K_m in 50 mM sodium acetate buffer (which included 1 μg/μl of BSA), pH 5.0, in a total volume of 140 μl, at 30 °C for 15 min. The reactions were stopped by adding 70 μl of 2 M sodium carbonate. The released *p*NP was quantified by measuring A_{405} and comparing it to that of a *p*NP standard curve. The V_{max}, K_m and k_{cat} were calculated from nonlinear regression of Michaelis–Menten plots with Grafit 5.0 software (Erithacus Software, Horley, UK).

For natural β-D-glucoside and glucooligosaccharide substrates, 0.01–1.0 μg of rOs4BGlu13 was incubated with concentrations of substrates that bracketed the apparent K_m in 50 mM sodium acetate buffer (which included 1 μg/μl of BSA), pH 5.0, in a total volume of 50 μl, at 30 °C for 15 min. The reactions were stopped by heating at 100 °C for 5 min (except for GA_4-GE, which was only heated 1 min), and then the released glucose was determined with the PGO assay as described above. The kinetic parameters were calculated as described for *p*NP glycosides.

2.9. Sequence analysis and homology modeling of Os4BGlu13

Secretory signal sequence prepeptide production was done with SignalP [32], while N-linked glycosylation sites were predicted with NetNGlc 1.0 [33]. Sequence alignments with closely related proteins were conducted with CLUSTAL 2.1 [34].

The Os3BGlu13 structure was modeled based on the structure of the closely related Os4BGlu12 [35]. Protein Data Bank Accession [PDB: 3PTK] was used as template for homology modeling and the three-dimensional model of Os4BGlu13 was generated by SWISS-MODEL via the ExPASy web server [36].

3. Results and discussions

3.1. Extraction, purification and characterization of GA_4-GE β-glucosidase from rice

Ten kilograms of 10-day rice seedling stems and leaves were extracted and the GA_4-GE β-glucosidase was purified with seven purification steps, while monitoring the activities for hydrolysis of *p*NPGlc and GA_4-GE (Table 1). Finally, 0.15 mg of protein was obtained after the seven steps of purification in which protein fractions with high hydrolysis activities toward GA_4-GE were pooled.

Table 1
Summary of purification of β-glucosidase in rice.

Purification step	Total activity (μmol/min.)		Protein (mg)	Specific activity (μmol/min.mg)		Purification fold		Yield[a] (%)
	*p*NP-Glc	GA_4-GE		*p*NP-Glc	GA_4-GE	*p*NP-Glc	GA_4-GE	
1. Crude extract	5710	11.0	27,200	0.21	$4.03 * 10^{-4}$	1	1	100
2. After (NH4)2SO4 precipitation & dialysis	2220	6.17	12,000	0.18	$5.12 * 10^{-4}$	0.9	1.3	56
3. CM-Sepharose 20 ml column	1470	4.22	1215	1.21	$3.47 * 10^{-3}$	5.8	8.6	38
4. Con A-Sepharose column	281	1.57	140	2.01	$1.12 * 10^{-2}$	9.6	27.8	14
5. Sephadex 75 column	157	1.50	57	2.73	$2.62 * 10^{-2}$	13	65	14
6. SP xl column	30.4	0.36	6	5.07	$6.0 * 10^{-2}$	24	149	3.3
7. Octyl column	3.07	0.05	0.63	4.88	$8.1 * 10^{-2}$	23	201	0.45
8. Superdex 200 column	1.63	0.02	0.15	10.9	0.136	52	337	0.18

4 mM *p*NPGlc and 1.72 mM of GA_4-GE were used for hydrolysis activity measurements.
[a] Yield was calculated based on GA_4-GE hydrolysis activity.

The purification of GA_4-GE-hydrolyzing β-D-glucosidase was 337 fold, while the recovery of activity was only 0.18%. During the purification, some of the enzyme molecules may have been degraded and lost their activity, which may be one main reason for the low purification yield. In addition, some isoenzymes that have GA_4-GE hydrolyzing ability (many with lower specific activity than the purified protein) were likely to have been removed during the purification, resulting in a decrease in yield.

3.2. Identification of β-glucosidase by LC-MS

Two major protein bands at approximately 60 kDa and 57 kDa were observed in SDS-PAGE of the final GA_4-GE β-glucosidase purified from rice (Fig. 2) and were identified by LC-MS of tryptic peptides generated from their SDS-PAGE gel bands. The peptide masses from the 60 kDa band matched Genbank accession EAZ01286.1, a hypothetical protein, OsI_23311 [*Oryza sativa* indica Group], with the matching score of 851. The peptide masses from the 57 kDa band matched Genbank accession NO_00105307.1, the protein product from the Os04g0474900 gene locus [*Oryza sativa* japonica Group], which corresponds to the glycoside hydrolase family GH1 β-glucosidase Os4BGlu13, with a matching score of 1006 and sequence coverage of 49%.

The 60 kDa protein OsI_23311 [*Oryza sativa* Indica Group] was predicted to have a molecular mass of 57,128 Da, and calculated pI of 8.67 for the precursor, including its signal peptide. The first 28 residues were predicted as a signal sequence in the precursor protein by SignalP 4.0 [32]; and 3 *N*-glycosylation sites at residues 33, 168 and 326 in the amino acid sequence of the precursor protein were predicted [33] (Supplementary Fig. S1). The molecular mass and theoretical pI of the mature protein were predicted to be 54,150 Da and 8.74, respectively. Since this protein bound to the Con A column, it is likely to be glycosylated, which may easily account for its slightly larger apparent size of 60 kDa on the SDS-PAGE. Although this protein is a member of the GlcD (**Genbank:** COG0277) family of FMN/FAD-containing dehydrogenases, the function of this protein is as yet unknown.

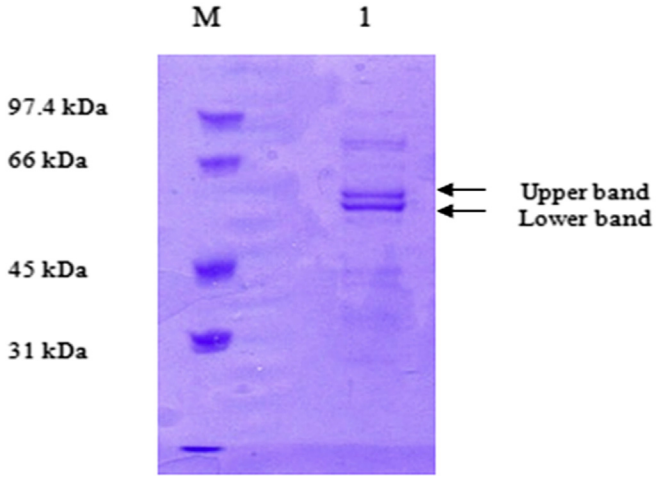

Fig. 2. 8% SDS-PAGE of fraction from Superdex S200 after staining with Coomassie brilliant blue. Lane M, protein marker; lane 1, purified fraction. The two major Coomassie-brilliant blue-stained bands were excised separately and submitted for tryptic digestion followed by LC-MS analysis.

The peptide masses from the 57 kDa protein matched the GH1 β-glucosidase Os4BGlu13. This precursor protein was calculated to have a molecular mass of 57,386 Da and pI of 6.44 when its signal peptide was included; and the molecular mass and theoretical pI after the signal peptide was removed were predicted to be 54,761 Da and 6.66, respectively. Considering the fact that there are five putative N-linked glycosylation sites in the amino acid sequence of the precursor protein, this molecular mass matched the size seen in the SDS-PAGE (Fig. 2).

The β-glucosidase Os4BGlu13, also called OsTAGG1, was previously reported by Wakuta et al. [4] as a β-D-glucosidase hydrolyzing tuberonic acid glucoside (TAG). The protein was previously purified from rice panicles by $(NH_4)_2SO_4$ fractionation and five different types of column chromatography. The purified OsTAGG1 migrated as a single band on native PAGE, but was present as two polypeptides with molecular masses of 42 kDa and 26 kDa under denaturing conditions. The two apparent subunits were caused by proteolytic cleavage of the initial mature protein to produce two bands in SDS-PAGE, based on the match of the two N-terminal sequences to the same gene. The sum of the molecular masses of the two polypeptides was 68 kDa, which is different from the predicted molecular mass of 55 kDa. This discrepancy was explained by authors as likely to be due to the fact that there are five *N*-linked glycosylation sites in the amino acid sequence of the precursor protein, so the molecular size of the mature protein could be increased by addition of sugar chains.

Our enzyme was extracted from 10-day old rice seeding stems and leaves, while the OsTAGG1 of Wakuta et al. [4] was extracted from rice panicles during grain filling. So, the different tissue sources may be the main cause for obtaining two different molecular sizes for the same mature protein, if the protein undergoes proteolytic processing in the panicle that does not occur in the seedling stems and leaves, and different levels of glycosylation occur in the different tissues. Since different purification methods were used, the previously purified OsTAGG1 may also have been proteolytically cleaved during the purification, while proteolysis at the same position did not appear to occur to the same extent in the current work, since the major Coomassie-brilliant-blue-stained band migrated at 57 kDa.

3.3. Hydrolysis activities of rOs4BGlu13 toward natural and synthetic glycosides

To test whether the Os4BGlu13 band was responsible for the GA_4-GE hydrolysis, we cloned the cDNA from rice seedlings and used it to express N-terminally thioredoxin-, His_6- and S-tagged fusion protein in *E. coli*. The Rosetta-gami(DE3) strain was found to give the best expression of four *E. coli* strains tested (also including BL21(DE3), Origami(DE3) and Origami B(DE3), data not shown). Although the expression level was low, such that the protein band was not obvious in the crude extract and the protein was still quite impure after the first IMAC step (Fig. 3), the two step IMAC purification provided 340-fold purification and 37% yield to give a protein with specific activity of 19.2 μmol/min/mg protein (Table 2). The purified Os4BGlu13 protein appeared as a single Coomassie brilliant blue stained band on SDS-PAGE, to allow further characterization (Fig. 3).

The rOs4BGlu13 was found to have high *p*NPGlc hydrolysis activity between pH 4.0 and 5.2, with highest value at pH 4.5, and with 50% of maximal activity at approximately pH 3.4 and 6.2 (Supplementary Fig. S2). This is similar to the pH optimum of approximately 4 reported for TAGG1 purified from rice panicle [4].

To evaluate the substrate specificity of the purified rOs4BGlu13, the hydrolysis activities of Os4BGlu13 toward natural and synthetic glycosides were determined (Table 3). Among *p*NP glycosides, rOs4BGlu13 had the highest hydrolysis activity toward *p*NPGlc, while *o*NPGlc gives only 18.8% of activity relative to *p*NPGlc, *p*NP-β-D-fucopyranoside yields 14.9% relative activity, and *p*NP-β-D-mannopyranoside, *p*NP-β-D-galactopyranoside, *p*NP-β-D-xylopyranoside gave relative activities of 4.4%, 1.5% and 0.7%, respectively.

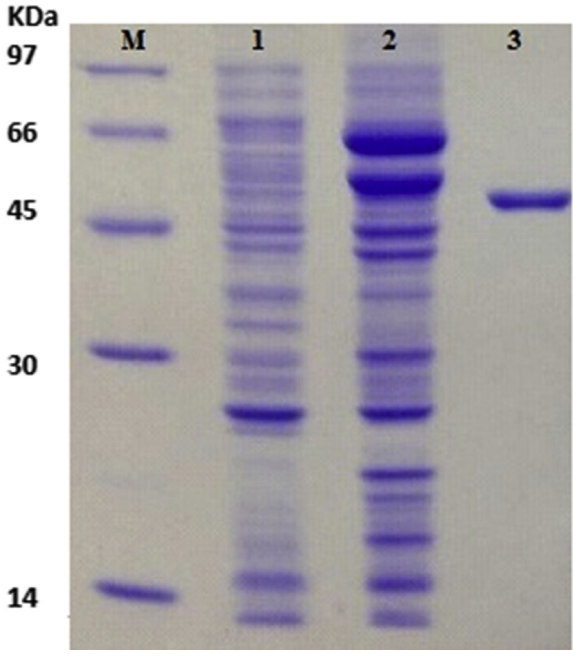

Fig. 3. SDS-PAGE profiles of Os4BGlu13 recombinant protein expressed in Rosetta-gami(DE3) *E. coli*. The 8% SDS-PAGE gel was stained with Coomassie brilliant blue. Lanes: M, standard marker (Bio-RAD); 1, Crude protein extract; 2, Protein purified by 1st immobilized metal affinity chromatography (IMAC); 3, The Os4BGlu13 protein after cutting off the fusion tags with enterokinase and removing them by a 2nd IMAC step.

Among glucooligo-saccharides, rOs4BGlu13 hydrolyzed laminaribiose [β-(1 → 3)-linked disaccharide] best (19.1% relative to *p*NPGlc), followed by laminaritriose (12.4%), cellotetraose (3.6%), cellotriose (2.0%) and cellopentaose (1.9%). rOs4BGlu13 could not hydrolyze longer β-(1 → 3) linked glucooligo-saccharides, such as laminaritetraose and laminaripentaose. By comparison, gentiobiose (6-O-β-D-glucopyranosyl-D-glucose was hydrolyzed with only 0.4% relative activity, although this was higher than the 0.1% of cellobiose. Thus, rOs4BGlu13 prefers short β-(1 → 3)-linked glucooligosaccharides.

Natural glycosides with different size of aglycones (Fig. 4) were compared to the putative natural substrates TAG and GA_4-GE (Table 3). The rOs4BGlu13 enzyme preferred smaller aromatic aglycones and with good leaving groups to large aglycones, especially those that are poorly ionized leaving group. Helicin (salicylaldehyde β-D-glucoside) gave the highest relative hydrolysis activity, followed by *n*-octyl-β-D-glucoside, D-amygdalin (D-mandelonitrile 6-*O*-β-D-glucosyl-β-D-glucoside), indoxyl β-D-glucoside, *n*-heptyl-β-D-glucoside, tuberonic acid glucoside (TAG), GA_4-GE, daidzein-7-O-β-D-glucopyranoside, salicylic acid glucoside (SAG) and methyl-β-D-glucoside. Hydrolysis of helicin results in release of salicylaldehyde, which is toxic to nematodes and bacteria and adapted by specialist insects as a defense compound [37]. The hydrolysis of daidzein, an isoflavonoid found in legumes, suggests that it may hydrolyze the structurally related flavonoid glycosides, although hydrolysis of the flavonoid apigenin 7-*O*-glucoside was very low. *Arabidopsis thaliana* BGLU15, which has been reported to fall in the same protein sequence-based phylogenetic cluster [28,38,39], has been shown to hydrolyze flavonoid glucosides that accumulate in vacuoles in response to abiotic stress [38].

The substrates *o*NPGlc, helicin, SAG have similar sized aglycones, but with different functional groups on the *ortho*-position of the phenyl ring. The pK_a values of the phenolic oxygen on these three aglycones are 7.2 for *o*NP, 8.2 for salicyladehyde and 13.8 for the salicylic acid. The hydrolysis activities of rOs4BGlu13 towards these three substrates are helicin > *o*NPGlc > SAG, which suggests the polarity of the *ortho* group may be more critical than the pK_a itself. Both daidzein-7-O-β-D-glucopyranoside and GA_4-GE have very large aglycones, which may limit the substrate binding to the active site, contributing to the low activities for these two substrates.

The kinetic parameters of Os4BGlu13 with substrates of interest are shown in Table 4. Its k_{cat}/K_m for *p*NPGlc (637 mM^{-1} s^{-1}) is highest, while that of *o*NPGlc is 8.5-fold lower and for *p*NP-β-D-fucopyranoside is over 30-fold lower. The k_{cat}/K_m for helicin is 74.4 mM^{-1} s^{-1}, which is 20-fold higher than the k_{cat}/K_m of GA_4-GE. Among the phytohormone glucoconjugates tested, TAG had the highest k_{cat}/K_m, while that of GA_4-GE was slightly lower and SAG was lowest. Among oligosaccharides, the most efficiently hydrolyzed oligosaccharide tested, laminaritriose, had a k_{cat}/K_m is

Table 2
Summary of purification of β-glucosidase from recombinant expression.

Purification step	Total activity (μmol/min.)	Protein (mg)	Specific activity (μmol/min.mg)	Purification fold	Yield[a] (%)
1. Crude extract	151	2674	0.0564	1	100
2. After first IMAC and buffer exchange	98.0	23.4	4.18	74	65
3. After second IMAC, buffer exchange and concentration	56.4	2.94	19.2	340	37

[a] Purification parameters were calculated based on *p*NPGlc hydrolysis activity.

Table 3
Relative activities of Os4BGlu13 toward natural and synthetic glycosides.

Substrates	Relative activity with standard deviation (%)
***p*NP glycosides**	
*p*NP-β-D-glucopyranoside	100 ± 1
*p*NP-β-D-fucopyranoside	14.9 ± 0.7
*p*NP-β-D-mannopyranoside	4.45 ± 0.12
*p*NP-β-D-galactopyranoside	1.48 ± 0.12
*p*NP-β-D-xylopyranoside	0.67 ± 0.12
*o*NP-β-D-glucopyranoside	18.8 ± 1.2
Glucooligosaccharides	
Laminaribiose [β-(1 → 3)-linked]	19.1 ± 3.5
Laminaritriose	12.4 ± 1.4
Laminaritetraose	0.73 ± 0.07
Laminaripentaose	0.19 ± 0.02
Cellobiose [β-(1 → 4)-linked]	0.13 ± 0.02
Cellotriose	1.99 ± 0.15
Cellotetraose	3.56 ± 0.18
Cellopentaose	1.90 ± 0.07
Cellohexaose	1.13 ± 0.14
Gentiobiose (6-*O*-β-D-Glucopyranosyl-D-glucose)	0.43 ± 0.03
Alkyl β-D-glucosides	
n-Octyl-β-D-glucoside	10.0 ± 0.5
n-Heptyl-β-D-glucoside	3.82 ± 0.29
Methyl-β-D-glucoside	0.42 ± 0.05
Natural β-D-glucosides	
Helicin (salicylaldehyde β-D-glucoside)	35.6 ± 2.2
D-Amygdalin (D-mandelonitrile 6-*O*-β-D-glucosido-β-D-glucoside)	9.60 ± 0.85
Indoxyl β-D-glucoside	8.93 ± 2.19
GA_4-GE (gibberellin A4 β-D-glucosyl ester)	1.54 ± 0.04
Tuberonic acid glucoside (TAG)	1.67 ± 0.02
Salicylic acid glucoside (SAG)	0.50 ± 0.003
Daidzin (daidzein-7-*O*-β-D-glucopyranoside)	0.54 ± 0.01
Apigenin 7-O-β-D-glucopyranoside	0.044 ± 0.004

1 mM substrates were used for relative activity measurement. The standard deviations were calculated based on three replicates.

5.57 mM^{-1} s^{-1}, which is lower than that of TAG, but higher than that of GA_4-GE. These data support the identification of Os4BGlu13 as a TAG β-glucosidase, but suggest it may play other functions in the plant as well, including helicin and perhaps GA_4-GE hydrolysis.

The hydrolysis of TAG, SAG and helicin by Os4BGlu13 support a role in wound response and regrowth, although *Os4BGlu13* gene expression is not induced in wounding [22]. Inspection of the microarray data in the Rice ExPro database [40] (http://ricexpro.dna.affrc.go.jp/field-development.php?featurenum=21285) indicates that the *Os4BGlu13* locus *Os4g0474900* is most highly expressed in root, leaf sheath during the vegetative stage and early stages of ovary growth. It is most highly expressed during the rapidly growing stage of roots (21–56 days after transplantation) and the expression drops off when root growth is essentially complete (63 days after transplantation). Since *Os4BGlu13* is most highly expressed in the development of roots, leaf sheath and ovary during their rapid growth, Os4BGlu13 hydrolysis of GA_4-GE may play a role in regulating growth in these tissues, although other Os4BGlu13 substrates may also be important in development of these tissues or providing for their defense.

3.4. Comparison of the protein structures and substrate binding for Os3BGlu6, Os3BGlu7, Os4BGlu12 and Os4BGlu13

To study the relationship between the protein structure and substrate binding, the amino acid sequences of Os3BGlu6, Os3BGlu7 and Os4BGlu12 were aligned with Os4BGlu13. The alignment in Fig. 5 shows that Os4BGlu12 and Os4BGlu13 have 85% identity, while Os3BGlu6 and Os3BGlu7 have 49% identity with Os4BGlu13 and each other.

The glutamate residues at positions 174 and 388 (Os4BGlu13 numbering) in the consensus sequences T(F/L)NEP and ITENG, respectively (Fig. 5), were predicted to be the acid-base catalyst and catalytic nucleophile, respectively, based on previous studies, including those on Os3BGlu6 [29], Os3BGlu7 [27] and Os4BGlu12 [28]. Although Os4BGlu12 and Os4BGlu13 have 85% amino acid sequence identity, these two enzymes have shown different specific activity, especially to GA_4-GE ester. The hydrolysis of GA_4-GE by partially purified Os4BGlu13 (approximately 50% purity from SDS-PAGE) was 1% of that of *p*NPGlc, while for recombinant Os4BGlu13 gave 1.5%. By comparison, the closely related Os4BGlu12 activity toward GA_4-GE was 0.03% of that toward *p*NPGlc, while Os3BGlu6, which had the highest relative activity compared to *p*NPGlc, had 7% [24]. Thus, relative to activity toward *p*NPGlc, the hydrolysis of GA_4-GE by Os3BGlu6 appears better than Os4BGlu13. However, the rOs4BGlu13 rate of hydrolysis of *p*NPGlc is quite high, similar to Os4BGlu12. In fact, the k_{cat}/K_m values of rOs4BGlu13, for both *p*NPGlc and GA_4-GE are much higher, 637 and 3.63 mM^{-1} s^{-1} respectively, compared to 6.2 and 0.13 mM^{-1} s^{-1} for Os3BGlu6, respectively [24]. Therefore, Os4BGlu13 is the most efficient enzyme for GA_4-GE hydrolysis among the enzymes that have been tested.

The four enzymes also showed different substrate preferences toward oligosaccharides. Os3BGlu7, Os4BGlu12 and rOs4BGlu13 hydrolyze β-(1,4)-linked oligosaccharides of 3–6 glucose residues, but differences were observed in their specificities for substrate chain lengths. The rates of hydrolysis of β-(1,4)-linked oligosaccharides by Os3BGlu7 increase with increasing chain length of the substrate, while those of Os4BGlu12 and rOs4BGlu13 remain approximately constant [24,25]. Os3BGlu6 had very low hydrolysis activities towards β-(1,4)-linked oligosaccharides [29]. Among the β-1,3-linked laminarioligosaccharides, Os4BGlu12 only hydrolyzes laminaribiose, while Os3BGlu6 Os3BGlu7, rOs4BGlu13 also hydrolyze laminaritriose, although at a lower rate than laminaribiose.

By comparing the active sites of Os3BGlu6, Os4BGlu12, and Os4BGlu13 (Fig. 6), we can see that the residues at the −1 site are

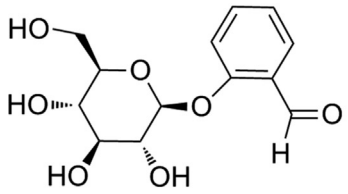

Helicin
(Salicylaldehyde beta-D-glucoside)

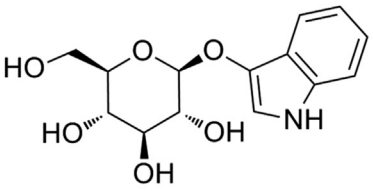

Indoxyl beta-D-glucoside

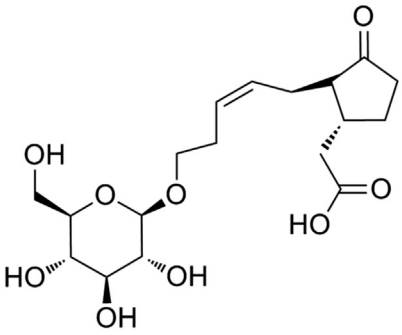

Tuberonic acid glucoside

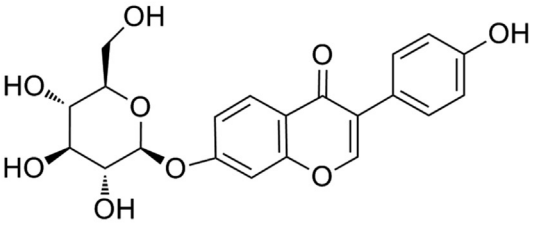

Daidzein-7-O-beta-D-glucoside

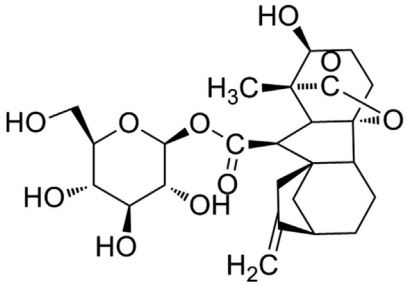

GA4-GE (gibberellin A4 beta
-D-glucosyl ester)

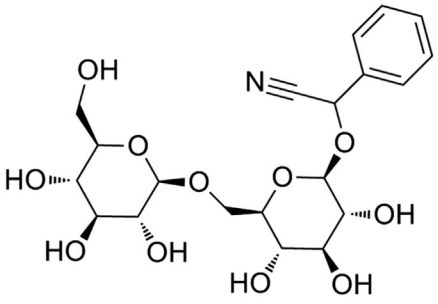

D-Amygdalin (D-Mandelonitrile 6-O-beta
-D-glucosido-beta-D-glucoside)

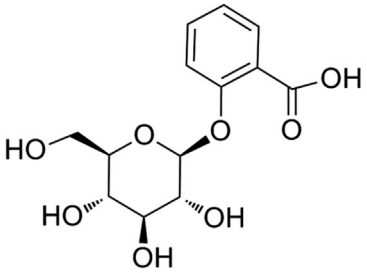

Salicylic acid glucoside

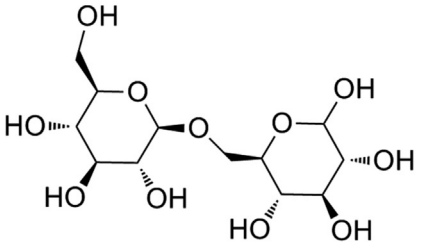

Gentiobiose (6-O-beta-D-glucopyranosyl-
beta-D-glucoside)

Fig. 4. Structures of natural β-D-glucoside substrates hydrolyzed by Os4BGlu13.

Table 4
Apparent kinetic parameters of Os4BGlu13 for hydrolysis of natural and synthetic glycosides.[a]

Substrate	V_{max}	K_m (mM)	k_{cat} (s^{-1})	k_{cat}/K_m (mM^{-1} s^{-1})
*p*NP-β-D-glucopyranoside	157 ± 7	0.234 ± 0.017	149 ± 8	637 ± 26
*p*NP-β-D-fucoside	3.87 ± 0.10	0.183 ± 0.016	3.68 ± 0.11	20.4 ± 4.0
*p*NP-β-D-mannoside	1.19 ± 0.03	1.22 ± 0.15	1.13 ± 0.03	0.927 ± 0.065
*p*NP-β-D-galactoside	3.69 ± 0.03	1.50 ± 0.10	3.51 ± 0.03	2.34 ± 0.17
*o*NP-β-D-glucoside	543 ± 2	7.19 ± 0.05	516 ± 2	71.8 ± 0.4
Helicin	65.4 ± 1.7	0.835 ± 0.065	62.1 ± 1.6	74.4 ± 2.6
Cellotriose	3.27 ± 0.02	1.90 ± 0.17	3.10 ± 0.02	1.64 ± 0.08
Cellotetraose	5.06 ± 0.07	3.44 ± 0.11	4.80 ± 0.07	1.39 ± 0.02
Cellopentaose	8.42 ± 0.03	4.71 ± 0.06	8.00 ± 0.06	1.70 ± 0.03
Laminaribiose	147 ± 2	31.8 ± 1.1	140 ± 2	4.40 ± 0.09
Laminaritriose	54.9 ± 1.2	9.36 ± 0.38	52.1 ± 1.2	5.57 ± 0.19
GA_4-GE	3.01 ± 0.05	0.788 ± 0.038	2.86 ± 0.04	3.63 ± 0.13
Tuberonic acid glucoside	2.86 ± 0.04	0.407 ± 0.026	2.71 ± 0.03	6.68 ± 0.34
Salicylic acid glucoside	1.58 ± 0.04	1.71 ± 0.09	1.50 ± 0.04	0.878 ± 0.022

[a] The values were derived from nonlinear regression of the Michaelis–Menton graphs and the standard errors are calculated from the curves, which included 3 replicates at no less than 6 substrate concentrations covering the range of at least 0.3 to 3 times the K_m.

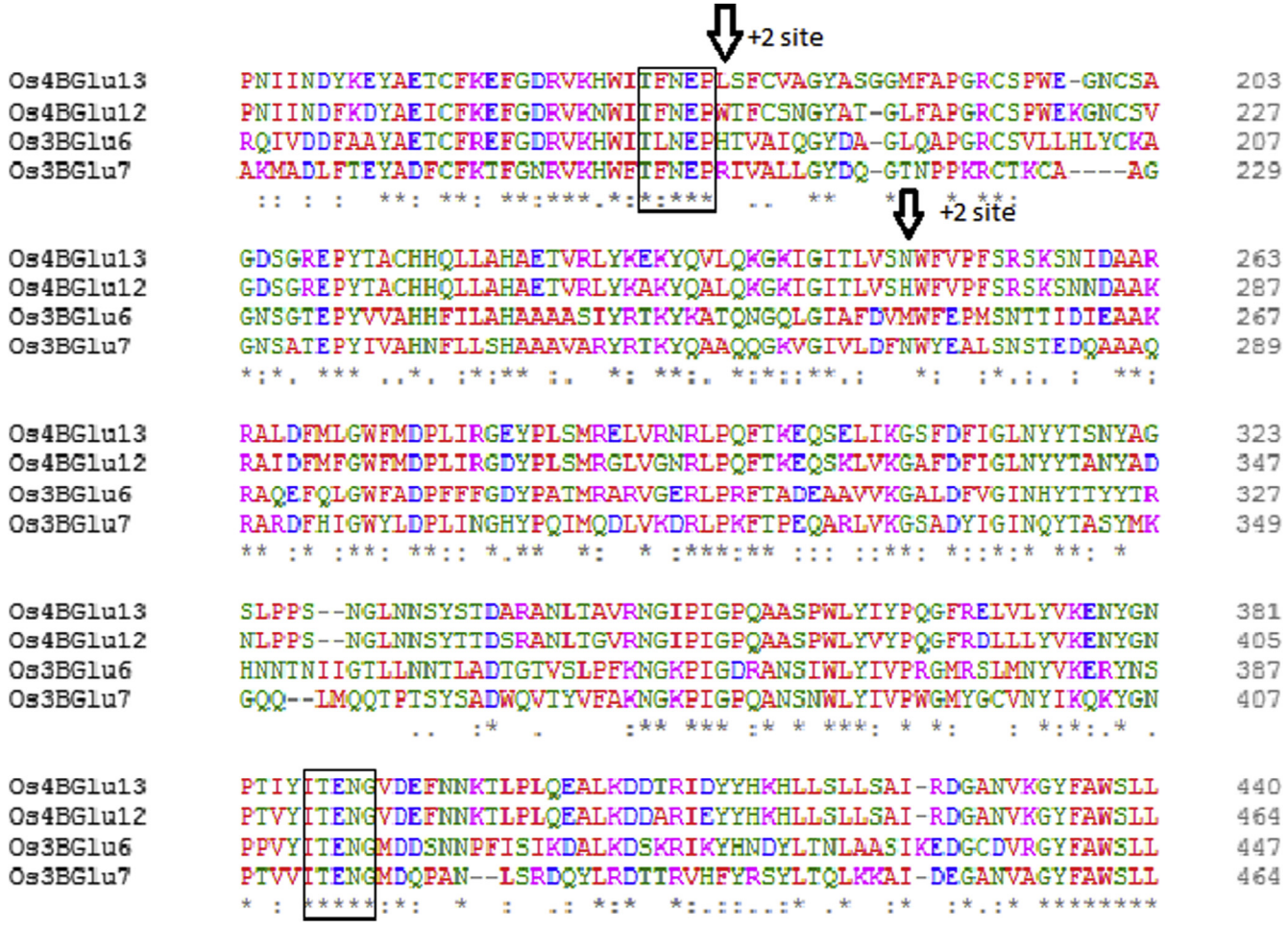

Fig. 5. Partial sequence alignment for four rice β-glycosidases, Os3BGlu6, Os3BGlu7, Os4BGlu12 and Os4BGlu13. The alignment was generated with Clustal 2.1 software [37]. The region shown includes the two catalytic amino acids, which fall in the consensus sequences that are boxed in rectangles, as well as most sugar-binding residues. The residues at the +2 site are indicated with black arrows.

well conserved for the three enzymes, but the residues at the +1 and +2 sites are different. For Os4BGlu12, two residues at the +2 site, W181 and H252, are bulkier and occupy more space than the residues at the same positions in Os3BGlu6 (H180 and M251) and Os4BGlu13 (L176 and N247), so they may lead to a smaller binding cleft. This may result in poor binding of GA_4-GE for Os4BGlu12, relative to Os4BGlu13 and Os3BGlu6, so that Os4BGlu12 hydrolyzed it poorly in comparison to Os4BGlu13 and Os3BGlu6.

This work suggested that the amino acid residues around binding cleft are very important for the substrate binding; the charge, the polarity and the sizes of the amino acid residues all contribute to the enzyme's substrate specificity. The enzymatic

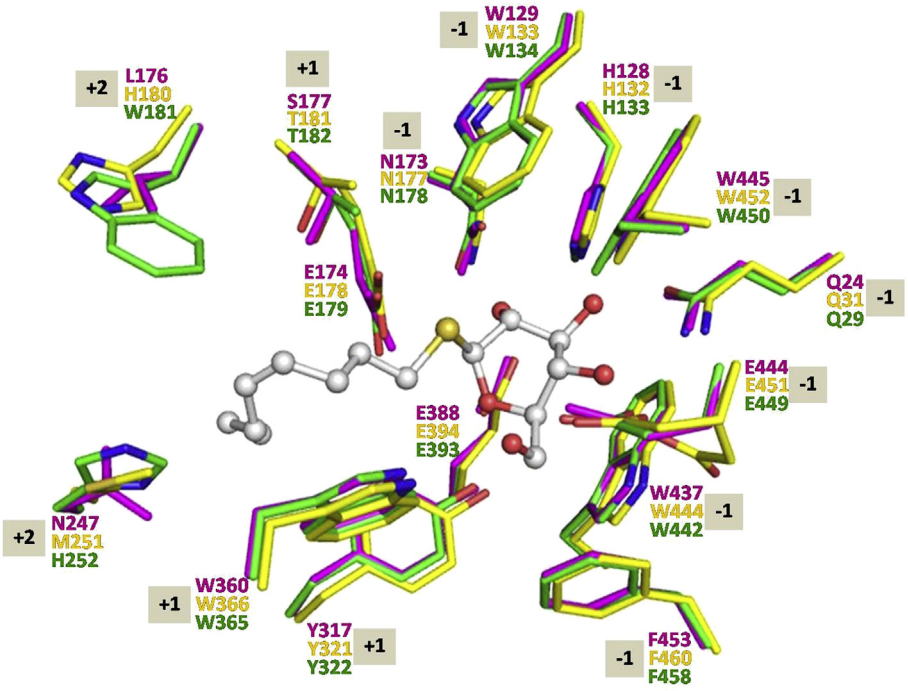

Fig. 6. The superimposition of the active sites of the Os3BGlu6 complex with *n*-octyl-β-D-thiogluco-pyranoside (PDB: 3GNP), Os4BGlu12 (PDB: 3PTK) and the homology model of Os4BGlu13. The carbons of octyl-β-D-thiogluco-pyranoside are gray, while the residues with pink carbons are from Os3BGlu13, those with yellow carbons are from Os3BGlu6 and those with green carbons are from Os4BGlu12. The subsites, relative to the positions of binding of β-1,4-linked glucosyl units, are indicated by the numbers (−1 for the nonreducing glucosyl residue, +1 for the next, and +2 for the next, going from the nonreducing to reducing end). The figures were generated by Pymol (Schrödinger LLC). An interactive version is available in the supplementary data as Fig. S3. (For interpretation of the references to color in this figure legend, the reader is referred to the web version of this article.)

data suggests that Os4BGlu13 may contribute to helicin, TAG, SAG, oligosaccharide and GA_4-GE hydrolysis in the rice plant. This may indicate a combined response including defense, wounding and systematic acquired resistance, recycling of damaged cell wall and regrowth, although such coordination of wounding response requires further study and other roles for Os4BGlu13 are possible.

Acknowledgments

We thank Ms. Chiraporn Saetang for assistance with protein purification and Ms. Daranee Chokchaichamnankit from the Chulabhorn Research Institute (CRI) and Ms. Atchara Paemanee from the National Center for Genetic Engineering and Biotechnology (BIOTEC) for their help on peptide analysis by LC-MS. This work was supported by Suranaree University of Technology (SUT1-102-55-36-01), the National Research University Project of the Commission on Higher Education of Thailand and the Thailand Research Fund (Grant BRG5680012).

Appendix A. Supplementary data

Supplementary data related to this article can be found at http://dx.doi.org/10.1016/j.abb.2015.07.021.

References

[1] W. Schliemann, J. Plant Physiol. 116 (1984) 123–132.
[2] K. Kai, K. Wakasa, H. Miyagawa, Phytochemistry 68 (2007) 2512–2522.
[3] K.H. Lee, H.L. Piao, H.Y. Kim, S.M. Choi, F. Jiang, W. Hartung, L. Hwang, J.M. Kwak, I.J. Lee, I. Hwang, Cell 126 (2006) 1109–1120.
[4] S. Wakuta, S. Hamada, H. Ito, H. Matsuura, K. Nabeta, H. Matsui, Phytochemistry 71 (2010) 1280–1288.
[5] P.J. Davies, Plant Hormones: Physiology, Biochemistry and Molecular Biology, Publisher, Kluwer Academic Publishes, 1995, ISBN 0792329848.
[6] J.D. Mauseth, Botany: an Introduction to Plant Biology, Saunders, Philadelphia, 1991, pp. 348–415.
[7] P.H. Raven, R.F. Evert, S.E. Eichhorn, Biology of Plants, Worth, New York, 1992, pp. 545–572.
[8] F.B. Salisbury, C.W. Ross, Plant Physiology, Wadsworth, Belmont, CA, 1992, pp. 357–407, 531–548.
[9] V.M. Sponsel, P. Hedden, in: P.J. Davies (Ed.), Plant Hormones: Biosynthesis, Signal Transduction, Action!, Kluwer, Dordrecht, 2004, pp. 62–98.
[10] G. Schneider, in: A. Crazier (Ed.), The Biochemistry and Physiology of Gibberellins, vol. 1, Praeger Publishers, New York, 1983, pp. 389–456.
[11] G. Schneider, E. Jensen, C.R. Spray, B.O. Phinney, Proc. Natl. Acad. Sci. U. S. A. 89 (1992) 8045–8048.
[12] M. Koshioka, E. Minami, H. Saka, R.P. Pharis, L.N. Mander, In: 13th International Conference on Plant Growth Substances, Edited by: R.P. Pharis and S. B. Rood, 217.
[13] T. Fowler, in: A. Esen (Ed.), Biochemistry and Molecular Biology, American Chemical Society, Washington DC, 1993, pp. 56–65. ACS Symposium Series 533.
[14] Y. Yildiz, H. Matern, B. Thompson, J.C. Allegood, R.L. Warren, D.M. Ramirez, R.E. Hammer, F.K. Hamra, S. Matern, D.W. Russell, J. Clin. Invest. 116 (11) (2006) 2985–2994.
[15] J.E. Poulton, Plant Physiol. 94 (1990) 401–405.
[16] L. Duroux, F.M. Delmotte, J.M. Lancelin, G. Keravis, C. Jay-Alleand, Biochem. J. 333 (1998) 275–283.
[17] B. Brzobohatý, I. Moore, P. Kristoffersen, L. Bako, N. Campos, J. Schell, K. Palme, Science 262 (1993) 1051–1054.
[18] A. Falk, L. Rask, Plant Physiol. 108 (1995) 1369–1377.
[19] D.P. Dharmawardhana, B.E. Ellis, J.E. Carlson, Plant Physiol. 107 (1995) 331–339.
[20] M. Reuveni, Z. Sagi, D. Evnor, A. Hetzroni, Plant Sci. 147 (1999) 19–24.
[21] L. Barleben, X. Ma, J. Koepke, G. Peng, H. Michel, J. Stöckigt, Biochim. Biophys. Acta 1747 (2005) 89–92.
[22] S. Wakuta, S. Hamada, H. Ito, R. Imai, H. mori, H. Matsuura, K. Nabeta, H. Matsui, J. Appl. Glycosci. 58 (2011) 67–70.
[23] K. Hiraga, T. Yokota, N. Takahashi, Phytochemistry 13 (1974) 2371–2376.
[24] Y. Hua, S. Sansenya, C. Saetang, S. Wakuta, J.R. Ketudat Cairns, Arch. Biochem. Biophys. 537 (1) (2013) 39–48.
[25] H. Matsuura, F. Ohmori, M. Kobayashi, A. Sakurai, T. Yoshihara, Biosci. Biotechnol. Biochem. 64 (2000) 2380–2387.
[26] G. Grynkiewicz, O. Achmatowicz, J. Hennig, J. Indulski, D.F. Klessig, Pol. J. Chem. 67 (1993) 1251–1254.
[27] R. Opassiri, J.R. Ketudat Cairns, T. Akiyama, O. Wara-Aswapati, J. Svasti, A. Esen, Plant Sci. 165 (2003) 627–638.

[28] R. Opassiri, B. Pomthong, T. Onkoksoong, T. Akiyama, A. Esen, J.R. Ketudat Cairns, BMC Plant Biol. 6 (2006) 33.
[29] S. Seshadri, T. Akiyama, R. Opassiri, B. Kuaprasert, J.R. Ketudat Cairns, Plant Physiol. 151 (1) (2009) 47–58.
[30] T. Kuntothom, S. Luang, A.J. Harvey, G.B. Fincher, R. Opassiri, M. Hrmova, J.R. Ketudat Cairns, Arch. Biochem. Biophys. 491 (1–2) (2009) 85–95.
[31] T.C. McIlvaine, J. Biol. Chem. 49 (1921) 183–186.
[32] T.N. Petersen, S. Brunak, G. von Heijne, H. Nielson, Nat. Methods 8 (2011) 785–786.
[33] R. Gupta, E. Jung, S. Brunak, NetNGlyc: Prediction of N-glycosylation Sites in Human Proteins, Software, 2005. http://www.cbs.dtu.dk/services/NetNGlyc/.
[34] M.A. Larkin, G. Blackshields, N.P. Brown, R. Chenna, P.A. McGettigan, H. McWilliam, F. Valentin, I.M. Wallace, A. Wilm, R. Lopez, J.D. Thompson, T.J. Gibson, D.G. Higgins, Bioinformatics 23 (2007) 2947–2948.
[35] S. Sansenya, R. Opassiri, B. Kuaprasert, C.J. Chen, J.R. Ketudat Cairns, Arch. Biochem. Biophys. 510 (2011) 62–72.
[36] M. Biasini, S. Bienert, A. Waterhous, K. Arnold, G. Studer, T. Schmidt, F. Kiefer, T. Gallo Cassarino, M. Bertoni, L. Bordoli, T. Schwede, Nucl. Acids Res. 42 (2014) W252–W258.
[37] P. Caboni, N. Aissani, T. Cabras, A. Falqui, R. Marotta, B. Liori, N. Ntalli, G. Sarais, N. Sasanelli, G. Tocco, J. Agric. Food Chem. 61 (2013) 1794–1803.
[38] J. Roepke, G.G. Bozzo, Phytochemistry 109 (2015) 14–24.
[39] C. Rouyi, S. Baiya, S.K. Lee, B. Mahong, J.S. Jeon, J.R. Ketudat-Cairns, M. Ketudat-Cairns, PLoS One 9 (2014) e96712.
[40] Y. Sato, H. Takehisa, K. Kamatsuki, H. Minami, N. Namiki, H. Ikawa, H. Ohyanagi, K. Sugimoto, B. Antonio, Y. Nagamura, Nucl. Acids Res. 41 (2013) D1206–D1213.